APPENDICES

Appendix Figures 1-5

Tables 1-3

Other Appendix Materials for this manuscript include the following:

“Appendix_Tables_3-28_Prikas-E_Thesis_PhD.xlsx”

Appendix Figures and Figure Legends

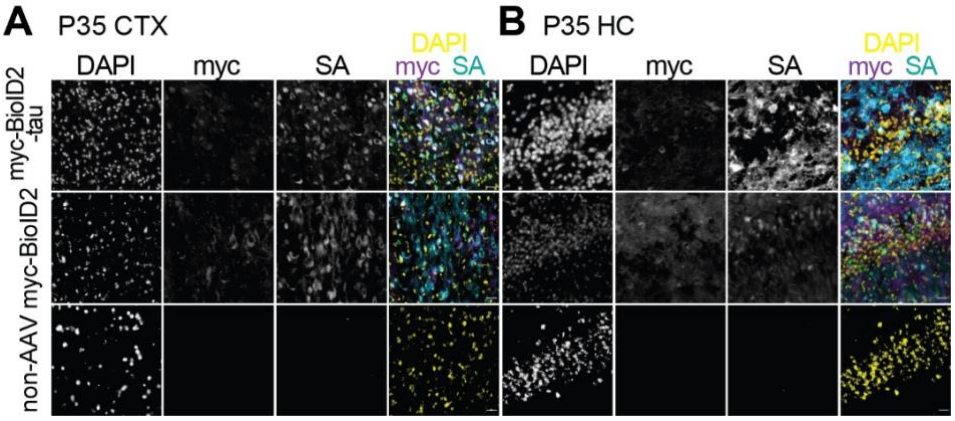

Appendix Figure S1. **Proximity labelling in *tau*$^{-/-}$ brain eliminates competition with endogenous tau for interaction partners and confirms tau associations with vesicular proteins**.

(**A-B**) Immunofluorescence of AAV-mediated BioID2-tau or BioID2 construct expression in mouse brain with channels detecting DNA (DAPI), BioID2-tau and BioID2 (myc), and biotinylated protein (SA). Representative images of P35 mouse brain cortex (CTX) (**A**) and hippocampus (HC) (**B**) infected with AAV at P0 and daily s.c. biotin on days P28-P35, (n = 3-5 per group, per condition). Scale bar, 50 µm.

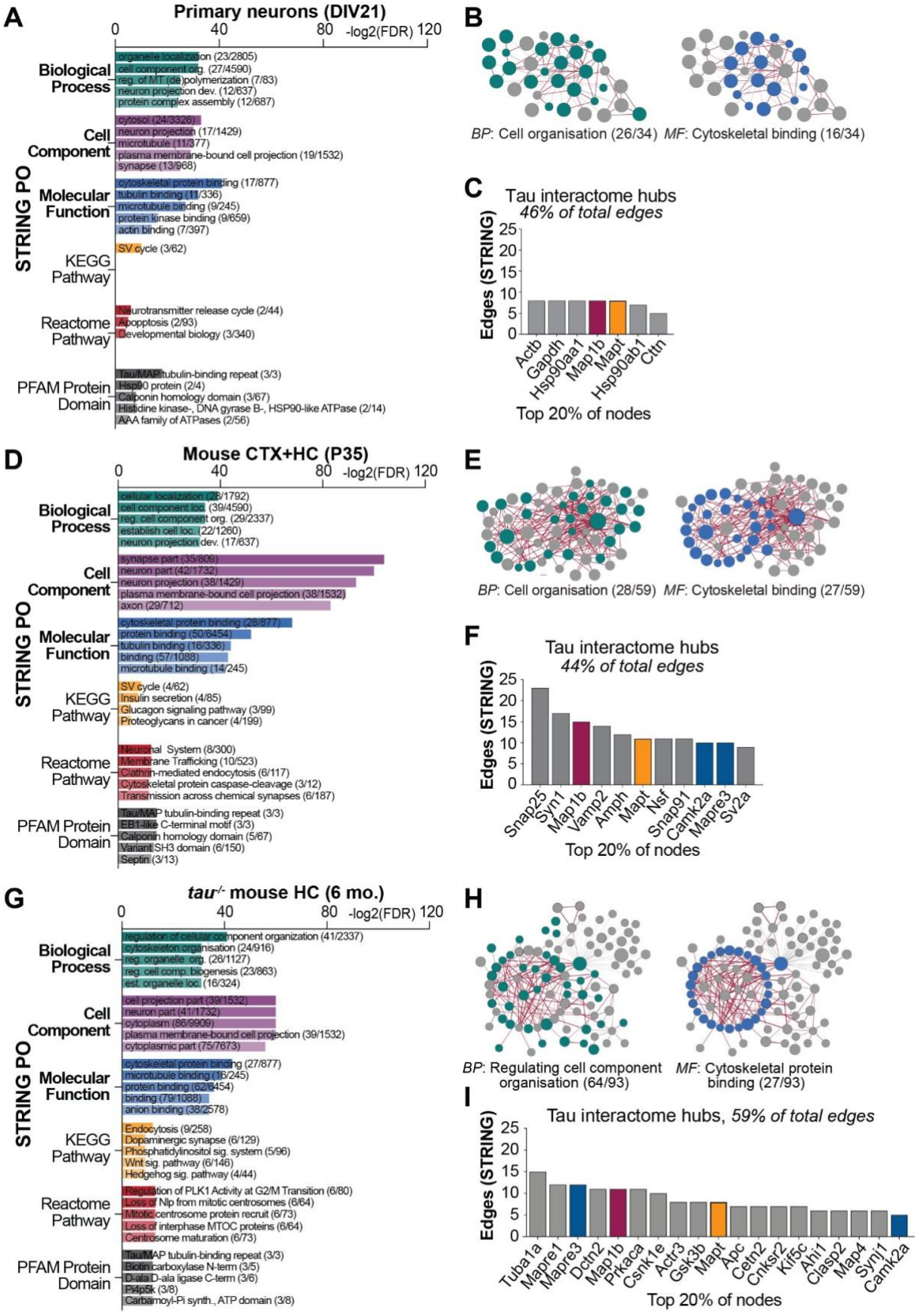
A
Primary neurons (DIV21)
0
40
80
-log2(FDR) 120
STRING PO
Biological Process
organelle localization (23/2805)
cell component org. (27/4590)
reg. of MT (de)polymerization (7/83)
neuron projection dev. (12/637)
protein complex assembly (12/687)
Cell Component
cytosol (24/3326)
neuron projection (17/1429)
microtubule (11/377)
plasma membrane-bound cell projection (19/1532)
synapse (13/968)
Molecular Function
cytoskeletal protein binding (17/877)
tubulin binding (11/336)
microtubule binding (9/245)
protein kinase binding (9/659)
actin binding (7/397)
KEGG Pathway
SV cycle (3/62)
Reactome Pathway
Neurotransmitter release cycle (2/44)
Apoptosis (2/93)
Developmental biology (3/340)
PFAM Protein Domain
Tau/MAP tubulin-binding repeat (3/3)
Hsp90 protein (2/4)
Calponin homology domain (3/67)
Histidine kinase-, DNA gyrase B-, HSP90-like ATPase (2/14)
AAA family of ATPases (2/56)
B
BP: Cell organisation (26/34)
MF: Cytoskeletal binding (16/34)
C
Tau interactome hubs
46% of total edges
Edges (STRING)
25
20
15
10
5
0
Actb
Gapdh
Hsp90aa1
Map1b
Mapt
Hsp90ab1
Cttn
Top 20% of nodes
D
Mouse CTX+HC (P35)
0
40
80
-log2(FDR) 120
STRING PO
Biological Process
cellular localization (28/1792)
cell component loc. (39/4590)
reg. cell component org. (29/2337)
establish cell loc. (22/1260)
neuron projection dev. (17/637)
Cell Component
synapse part (35/809)
neuron part (42/1732)
neuron projection (38/1429)
plasma membrane-bound cell projection (38/1532)
axon (29/712)
Molecular Function
cytoskeletal protein binding (28/877)
protein binding (50/6454)
tubulin binding (16/336)
binding (57/1088)
microtubule binding (14/245)
KEGG Pathway
SV cycle (4/62)
Insulin secretion (4/85)
Glucagon signaling pathway (3/99)
Proteoglycans in cancer (4/199)
Reactome Pathway
Neuronal System (8/300)
Membrane Trafficking (10/523)
Clathrin-mediated endocytosis (6/117)
Cytoskeletal protein caspase-cleavage (3/12)
Transmission across chemical synapses (6/187)
PFAM Protein Domain
Tau/MAP tubulin-binding repeat (3/3)
EB1-like C-terminal motif (3/3)
Calponin homology domain (5/67)
Variant SH3 domain (6/150)
Septin (3/13)
E
BP: Cell organisation (28/59)
MF: Cytoskeletal binding (27/59)
F
Tau interactome hubs
44% of total edges
Edges (STRING)
25
20
15
10
5
0
Snap25
Syn1
Map1b
Vamp2
Amph
Mapt
Nsf
Snap91
Camk2a
Mapre3
Sv2a
Top 20% of nodes
G
tau-/- mouse HC (6 mo.)
0
40
80
-log2(FDR) 120
STRING PO
Biological Process
regulation of cellular component organization (41/2337)
cytoskeleton organisation (24/916)
reg. organelle org. (26/1127)
reg. cell comp. biogenesis (23/863)
est. organelle loc. (16/324)
Cell Component
cell projection part (39/1532)
neuron part (41/1732)
cytoplasm (86/9909)
plasma membrane-bound cell projection (39/1532)
cytoplasmic part (75/7673)
Molecular Function
cytoskeletal protein binding (27/877)
microtubule binding (16/245)
protein binding (62/6454)
binding (79/1088)
anion binding (38/2578)
KEGG Pathway
Endocytosis (9/258)
Dopaminergic synapse (6/129)
Phosphatidylinositol sig. system (5/96)
Wnt sig. pathway (6/146)
Hedgehog sig. pathway (4/44)
Reactome Pathway
Regulation of PLK1 Activity at G2/M Transition (6/80)
Loss of Nlp from mitotic centrosomes (6/64)
Mitotic centrosome protein recruit (6/73)
Loss of interphase MTOC proteins (6/64)
Centrosome maturation (6/73)
PFAM Protein Domain
Tau/MAP tubulin-binding repeat (3/3)
Biotin carboxylase N-term (3/5)
D-ala D-ala ligase C-term (3/6)
PI4p5k (3/8)
Carbamoyl-PI synth., ATP domain (3/8)
H
BP: Regulating cell component organisation (64/93)
MF: Cytoskeletal protein binding (27/93)
I
Tau interactome hubs, 59% of total edges
Edges (STRING)
25
20
15
10
5
0
Tuba1a
Mapre1
Mapre3
Dctn2
Map1b
Prkaca
Csnk1e
Actr3
Gsk3b
Mapt
Apc
Cetn2
Cnksr2
Kif5c
Ahi1
Clasp2
Map4
Synj1
Camk2a
Top 20% of nodes

Appendix Figure S2. **Characteristics of network analyses, protein ontology and network hub identities across tau interactomes.**

(**A-C**) Horizontal bar graphs summarizing protein ontology (PO) analyses from each tau interactome as identified using STRING database (v11.5). Top five results from each category are shown, based on the False Discovery Rate (*FDR*).

(**D-F**) Bar graphs indicating the 20% most interconnected nodes (hubs) from each network, colour-coded to show overlap (co-identification) across networks.

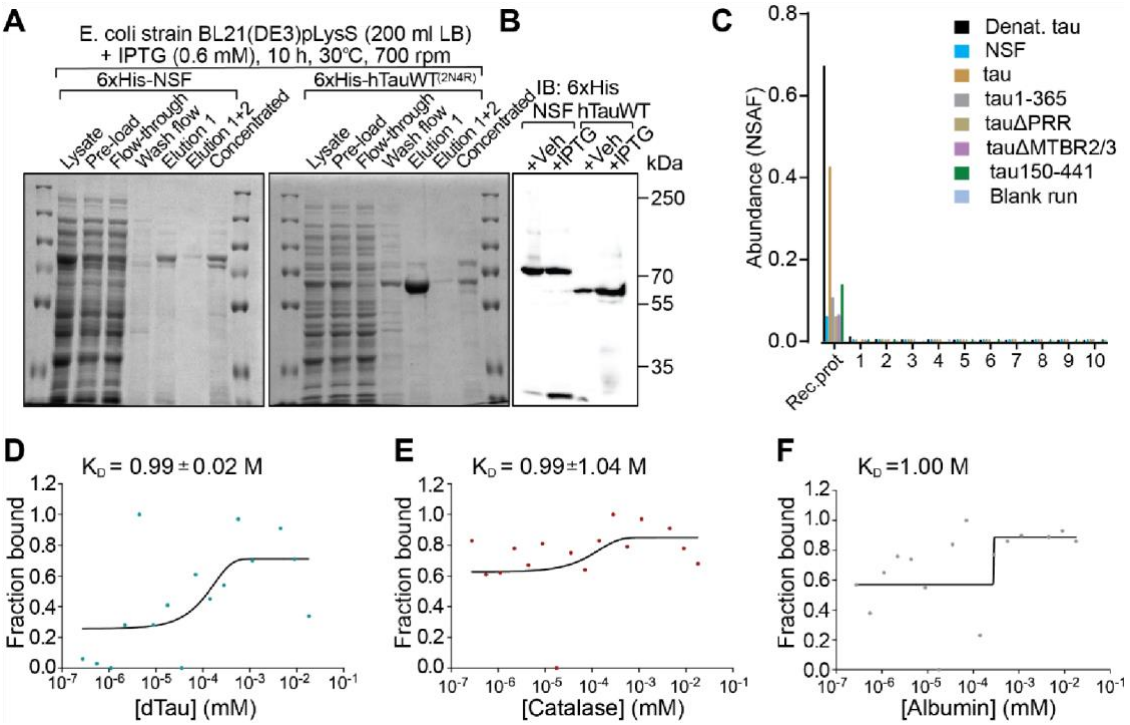

Appendix Figure S3. **Characteristics of protein preparations and control binding curves in microscale thermophoretic measurements.**

(**A-C**) Purification of recombinant human NSF and tau for MST assay (*see Figure 2H*) and ATPase assays (*see Figures 3A, S3A-H*). Coomassie gels' lane seven correspond to immunoblot lanes '+IPTG' and contain 2 µg of purified protein. (**A**) Coomassie blue staining of protein separated on 10% SDS-PAGE gels. Recombinant protein purification from bacterial lysate at seven stages of purification for humanized NSF 744 aa (left) and tau isoform 441 aa (right) (**B**) Immunoblot shows comparison between purified 6xHis-tagged NSF and tau from non-induced or IPTG-induced bacteria (**C**) Analysis of recombinant protein preparations used in this study showing abundance of isolated protein and first 10 co-detected protein IDs. Abundance is estimated by normalized spectra-associated factor (NSAF). Protein scores of recombinant proteins range from 700-1,400, whereas co-detected protein IDs were ~30-50.

(**D**-**F**) Microscale thermophoretic (MST) measurement of recombinant proteins (18 mM – 0.275 nM) and recombinant hexameric NT-647-NHS-labelled NSF (27 pM), (*see Figure 2H*). (**D**) MST binding curve of denatured tau (95 C, 5 min) and NSF. Dissociation constant: K_D = 0.99 ± 0.02 M (sigmoidal curve fit, R^2 = 0.358). (**E**) MST binding curve of catalase and NSF. Dissociation constant: K_D = 0.99 ± 1.04 M (sigmoidal curve fit, R^2 = 0.193). (**F**) MST binding curve of albumin and NSF. Dissociation constant: K_D = 1.00 M, no calculable ± confidence interval value (sigmoidal curve fit, R^2 = 0.296). (n = 1 per condition). Values are dissociation constant ± 95% confidence intervals (CI).

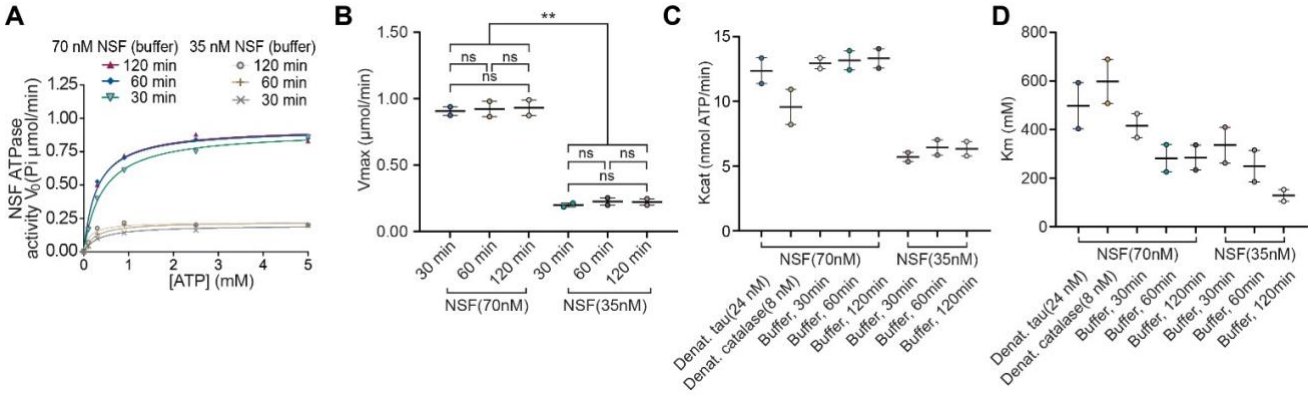

Appendix Figure S4. **Baseline ATPase activity of recombinant NSF**

(**A**) Optimization of assay conditions for determination of NSF k_{cat} values. For an ATP concentration range of 0-5 mM, the asymptotic V_{max} values indicated that 60 min was an appropriate incubation time, measuring activity of NSF at 70 nM.

(**B**) Maximal rate of phosphate (Pi) generation was significantly higher in assays containing 70 nM of NSF relative to 35 nM NSF, irrespective of incubation time (30-120 min).

(**C-D**) Rate constants were derived from kinetic data in A. (**C**) Catalytic rate of ATP hydrolysis was similarly higher in 70 nM NSF with or without 24 nM dTau compared to 35 nM NSF. (**D**) Bar graph representation of NSF K_m values under various indicated conditions. Rate of ATP hydrolysis was determined by measuring generation of Pi using Malachite Green Assay. Starting ATP concentrations were: 0, 0.3125, 0.625, 1.25, 2.5, and 5 mM at 30/60/120 min incubation times. Kinetics values were determined using non-linear fit (R^2 = 0.946 – 0.997 for all ATPase assays).

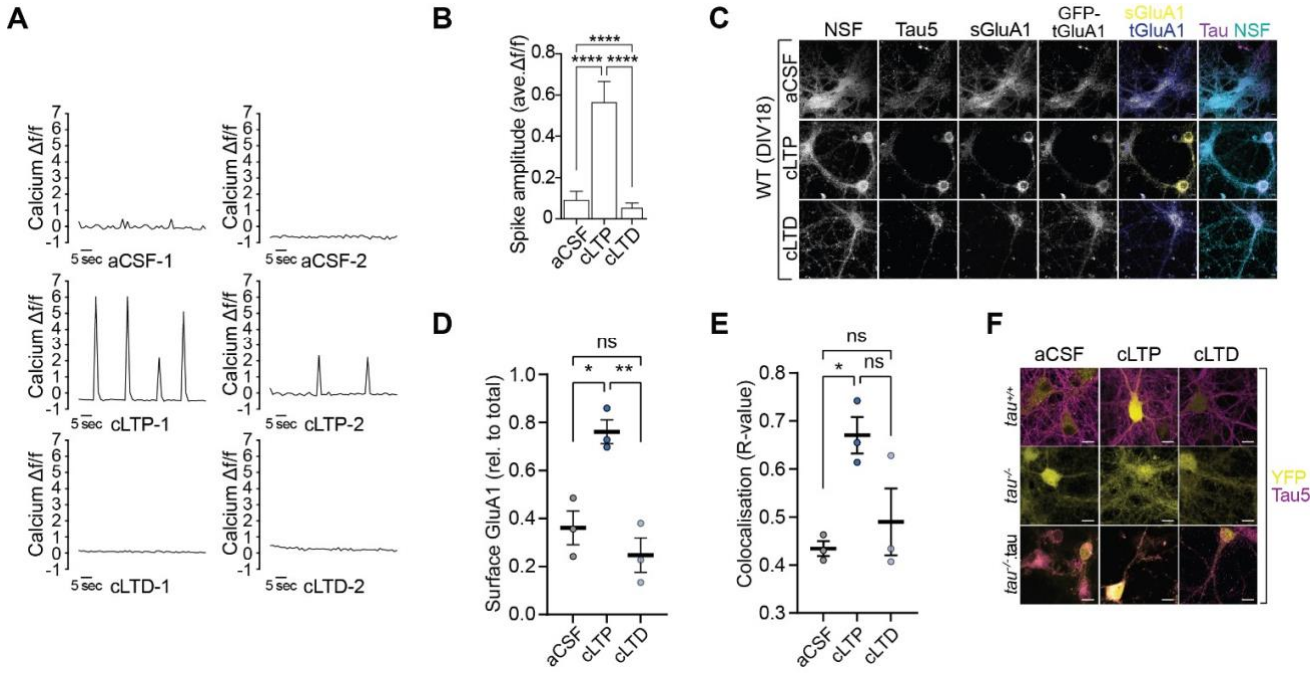

Appendix Figure S5. **Characterization of modified aCSF to induce chemical LTP and LTD**.

(**A**) Live cell calcium transients from neurons expressing GCaMP6f. Trace patterns of calcium induced fluorescence is most apparent in cLTP-induced neurons. Average baseline fluorescence is higher in cLTD-induced neurons compared to aCSF

controls. Recordings are from ~50 neurons, n = 2 per condition.

(**B**) Average spike amplitude of calcium-dependent fluorescence is significantly higher in neurons incubated with aCSF

for chemical LTP.

(**C**-**E**) Primary hippocampal neurons fixed 90 min after cLTP or cLTD. (**C**) Representative immunofluorescent images (n = 4) showing neurons transfected with GFP-GluA1 (blue) at DIV7 and probed for NSF (cyan), tau (magenta), and surface GluA1 (yellow). Rows 6 and 7 show yellow-blue overlap of surface and total GluA1, and magenta-cyan overlap of tau-NSF. Scale bar, 5 μm. (**D**) Increased surface GluA1 levels relative to total (GFP-GluA1) in cLTP-induced primary neurons. (**E**) Increased colocalization of tau with NSF in cLTP-induced primary neurons relative to treatment controls.

(**F**) Tau expression levels are consistent with reported genotypes and conditions. Neurons were transduced with AAV^{cFosYFP} at DIV7 and some *tau*$^{-/-}$ neurons transfected with TauV5 at DIV12. Cells fixed on DIV18 at 2 h post-treatment were stained for tau (magenta). YFP signal (yellow) generated from native expression of fluorescent protein. Scale bar, 10 μm.

Values are means ± S.E.M. Adjusted p-values: ****p < 0.0001, **p < 0.01, *p < 0.05, ns, not significant, ANOVA with nonparametric Dunn's test in B and Sidak's test in D and E

Appendix Tables

Table 1. **Biotinylation in C57Bl/6 cortical primary neurons (DIV21), and in mouse brain of C57Bl/6 (P35) and *tau*$^{-/-}$ (6 mo.) strains.** Biotinylated peptides/proteins detected by mass spectrometry from enriched lysates.

Summary table is based on lists of peptides found in Table

	Primary Neurons (DIV21)		CTX and HC (P35)		HC tau-/- (6 m.o.)	
	myc-BioID2 n = 3	myc-BioID2-tau n = 3	myc-BioID2 n = 12	myc-BioID2-tau n = 12	myc-BioID2 n = 6	myc-BioID2-tau n = 6
Total biotinylated peptides	187	357*	223	712*	1288	1191*
Total unique biotinylated proteins	65	94	47	101	316	210
Network proteins	NA	34	NA	59	NA	93

*CTX = cortex; HC = hippocampus; P35 = post-natal day 35; 6 mo. = 6 months old. *Does not include biotinylated peptides from humanized tau or endogenous mouse tau*.

Table 2. **Biotinylated mouse tau peptides**. Biotinylated tau peptide fragments in primary mouse cortical (CTX) neurons and in post-natal day 35 (P35) mouse brain (CTX and hippocampal (HC)) expressing BioID2-hTau.

Example biotinylated peptide sequences are exclusive to endogenous mouse tau.

Sample	Expression model	Peptide Score	Biotinylated Mouse Tau Peptide
A	Primary neurons	40.06	GADG**K**TGAK
A	Primary neurons	77.52	TGA**K**IATPR
A	Primary neurons	62.73	IPA**K**TTPSPK
B	P35 CTX+HC	43.93	TPPGSGEPP**K**SGER
C	P35 CTX+HC	57.59	TPP**K**SPSASK
D	P35 CTX+HC	43.93	TTPSP**K**TPPGSGEPPKSGER
E	P35 CTX+HC	41.91	VAS**K**DR
F	P35 CTX+HC	56.38	GTSNATRIPA**K**TTPSPK

Bold, red, underlined 'K' denotes biotinylated lysine residue

Table 3. **Biotinylated tau interactor proteins**. 260 unique biotinylated proteins were identified across 3 biological expression systems using BioID2-tau. Expression systems were (1) primary cortical mouse neurons, (2) P35 mouse cortex and hippocampus, and (3) 6 mo. *tau*$^{-/-}$ mouse hippocampus. The number of proteins that appeared in more than one system are shown.

Biotinylated protein overlaps			
***tau*$^{-/-}$ + P35 + Primary**	***tau*$^{-/-}$ + P35**	***tau*$^{-/-}$ + Primary**	**P35 + Primary**
50/260 (19.2%)	29/260 (11.2%)	14/260 (5.4%)	5/260 (2.3%)